Degradation of Radiometers in Space: Application to VIRGO TSI

Claus Fröhlich
VIRGO Data Analysis Center
CH-7265 Davos Wolfgang, Switzerland

July 6, 2014

Abstract

A degradation model is presented which depends on the dose as determined from the MgII index and on instrument's temperature. This model can be applied to correct the VIRGO Radiometers and Sunphotometers for long-term changes. The method presented is used since version 6.4.

1 Model for the Long-Term Changes of the VIRGO Radiometers and Sunphotometers

The simple model for the long-term changes is based on the effect which describes the sunburn of quartz by dissociation of SiO_2 at the surface. The solar photons – mainly from Ly-α – reduce the surface SiO_2 leaving a layer of silicon. This layer then absorbs the impinging photons and protects the remaining SiO_2 from further damage. The thickness y of the silicon layer grows with time t due to irradiance by UV photons with the wavelength λ_0 according to

$$\frac{dy}{dt} = \sigma_0 F_0 a \exp\left(-\kappa_0 y\right), \tag{1}$$

with a the thickness (m) of a monolayer of Si, and with σ_0 the cross section (m^2) for a UV photon to produce Si from SiO_2, F_0 the irradiance (photons/m^2/s) and κ_0 the absorption coefficient (m^{-1}) of the Si film at the wavelength λ_0. With $y = 0$ at $t = 0$ the solution is

$$y = \frac{1}{\kappa_0} \ln\left(1 + a\kappa_0\sigma_0 F_0 t\right), \tag{2}$$

indicating a logarithmic slow down of an initial linear rise. The transmission $\mathcal{T}_\lambda$ at the wavelength λ with corresponding absorption coefficient κ_λ, which determines the exposure-dependent changes of optical surfaces at this wavelength, becomes

$$\mathcal{T}_\lambda = \left(1 + a\kappa_0\sigma_0 F_0 t\right)^{-\frac{\kappa_\lambda}{\kappa_0}}. \tag{3}$$

Thus, this effect is described by a power law and the exponent depends on the ratio of the absorption coefficients at the dominant wavelength λ and the time dependent change corresponds to a time constant $\tau = 1/\left(a\kappa_0\sigma_0 F_0\right)$. As F_0 depends on time through the varying amount of UV irradiance with time $F_0 t$ needs to be replaced by $F_0 D(t_{\rm exp})$. With $t_{\rm exp}$ being the time during exposure to $\lambda m(t)$ the varying UV irradiance from the Sun, $D(t_{\rm exp})$ becomes now

$$D(t) = \int_0^t (1 + \lambda m(t)) dt_{\rm exp} = t_{\rm exp} + \int_0^t \lambda m(t) dt_{\rm exp}. \tag{4}$$

The normalized MgII index $(0 \ldots 1)$ is used as proxy for the UV irradiance and is shown in Fig. 1 for the last three solar cycles.

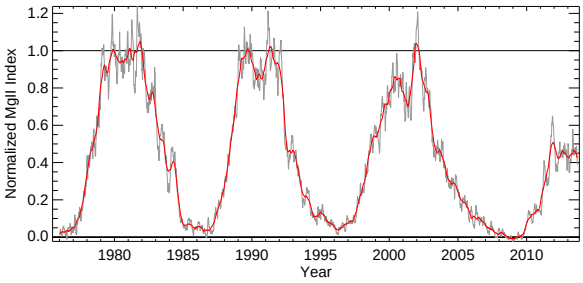

Figure 1: *Time-series $m(t)$ of the normalized MgII index as proxy for solar UV irradiance determining the dose.*

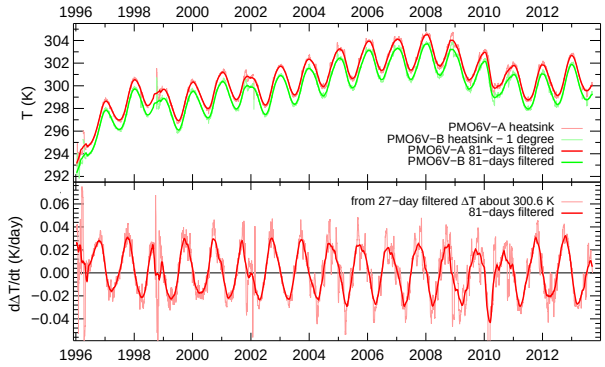

Figure 2: *The top panel shows $T(t)$ of the heat sink temperatures of PMO6V-A and B and the bottom panel the first derivative of the average $\Delta T(t)$, filtered with 27-day boxcar.*

The time-dependent correction $C(t)$ for the change in sensitivity of a radiometer starting with 0 at $t = 0$ becomes now

$$C(t) = c\left[\left(1 + \frac{D(t)}{b\tau_C}\right)^{-b} - 1\right] \tag{5}$$

with $\frac{1}{b\tau_C}$, b, c and λ adjustable parameters. The b is added as a factor to τ_C in order to corresponds to an $1/e$ time constant.

Table 1: *In order to compare the functions according to Eq. 5 and Eq. 6 a hyperbolic function is created according to Eq. 5 with the parameters $c = 1.0$, $\tau_c = 50$days, and $\lambda = 0.5$ and fitted with an exponential function according to Eq. 6. The results from Eq. 6 yield reasonably accurate results, although the coefficient differ at low b values.*

b	c	τ_c	λ	Deviation
0.5	0.3609	27.39	1.2749	1701.5 ppm
1.0	0.5602	35.08	0.8726	1668.8 ppm
2.0	0.7856	43.11	0.6381	1726.8 ppm
4.0	0.9792	49.51	0.5081	1715.2 ppm
8.0	0.9957	49.95	0.5003	908.1 ppm
16.0	0.9979	49.98	0.5002	455.1 ppm
32.0	1.0000	50.00	0.5000	929.3 ppm

For large b the hyperbolic function goes over to an exponential one (see 5.2.3 Deutschschweizerische Mathematik- und Physikkommission, 1997) which will be used in further analysis

$$C(t) = c\left[\exp\left(-\frac{D(t)}{\tau_C}\right) - 1\right]. \tag{6}$$

Table 1 shows the results of a hyperbolic function with $c = 1$, $\tau_C = 50.$ and $\lambda = 0.5$ for the different b, fitted to an exponential according to Eq. 6. The fit gives reasonably small overall deviations, but the coefficients are underestimated for b values < 8.0. For larger time constants as e.g. 500 days the turnover is already at $b = 1.0$, for shorter ones as e.g. 20 days the turnover is between $b = 16$ and 32. The conclusion is that the exponential function can be used even in the case of a small exponent, but the values of the coefficients deviate from the physical meaning as defined by the hyperbolic function and the corresponding differential equation.

During the analysis of the VIRGO SPM it became clear (see Fig. 3) that also the degradation depends on temperature. The first idea was a Boltzmann factor $\exp\left(-\frac{E}{kT}\right)$ which describes the temperature dependence of a reaction rate or for the degradation the ratio $m(t,T)/m(t,T_0) = \exp\left(-\frac{E}{kT} + \frac{E}{kT_0}\right)$. With T_0, a reference temperature and $\frac{E}{kT} = \frac{E}{kT_0}(1 - \frac{T-T_0}{T_0})$

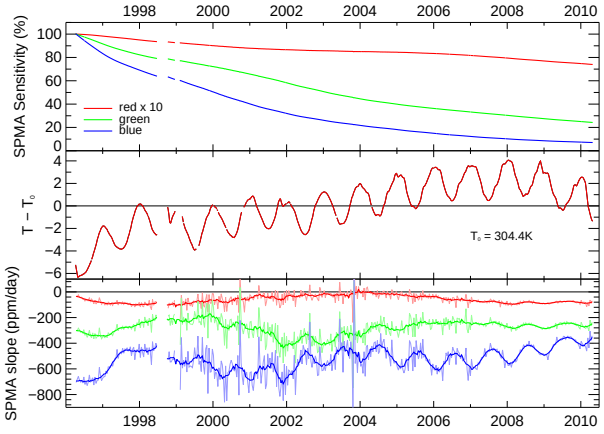

Figure 3: *Top panel: Sensitivity change of the three operational VIRGO/SPM. The temperature dependence of the sensitivity has been removed. Middle panel: Temperature of the operational VIRGO/SPM. Bottom Panel: Slope of the sensitivity change in ppm/day which obviously depends not only on the dose, but also on temperature. Note that higher temperatures result in steeper (more negative) slope.*

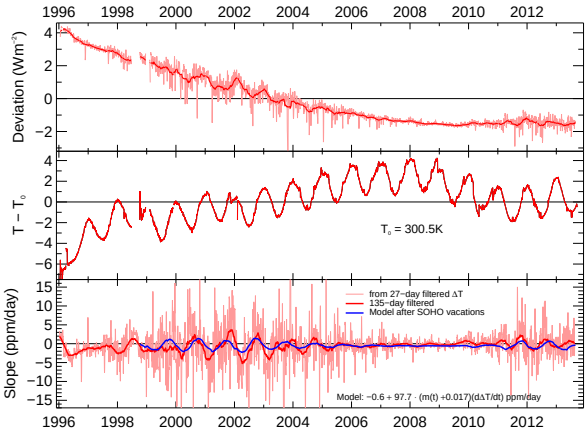

Figure 4: *Top panel: Sensitivity change of PMO6V-A. Middle panel: Temperature of the the heat sink of PM6V-A. Bottom Panel: Slope of the sensitivity change in ppm/day which also shows the temperature dependence. Moreover, the model of Eq. 10 can indeed explain this effect.*

the ratio becomes $\exp\left(\frac{E(T-T_0)}{kT_0^2}\right)$ or $\left(1+\frac{E(T-T_0)}{kT_0^2}\right)$. With $\Delta T = T - T_0$ the temperature dependent contribution of the UV radiation to the dose is $m(t,T) = m(t,T_0)(1+\alpha\Delta T)$ with $\alpha = \frac{E}{kT_0^2}$. At room temperature the 'doubling-every-ten-degrees' corresponds to $\frac{E}{kT} = 0.72$ or to an activation energy of about 0.02 eV. Even with an activation energy as high as 2 eV α is only about 0.002 per degree and with a range of $\pm 4.5°$ at most a percent of the normalized $m(t)$. So, the Boltzmann effect is too small to explain the observed temperature modulation of the slope and hence, it has to be a more direct effect on the degradation function. Thus, $D(t)$ does not have a temperature effect, but a possible 'recovery' during non-exposed periods should be included, leading to

$$D(t) = \int_0^t dt_{\rm exp} + \lambda \int_0^t m(t_{\rm exp}) dt_{\rm exp} - r_0 \int_0^t dt_{\rm nexp}. \tag{7}$$

Form the above discussion the temperature influence should be included in Eq.6 with a term $(1+\alpha\Delta T)$ and $\Delta T = T - T_{\rm ref}$ with $T_{\rm ref}$ being e.g. the mean temperature over the mission:

$$C(t) = c\left[(1+\alpha\Delta T(t))\exp\left(-\frac{D(t)}{\tau}\right) - (1+\alpha\Delta T(0))\right]. \tag{8}$$

The SPM green channel and less obvious also the PMO6V (Fig. 4) suggest that this modulation depends also on the dose which can be included by adding to α a term $(\beta m(t) + (1-\beta)$ with $0 < \beta < 1$ being the fraction of the cycle modulation. Eq. 10 becomes now

$$C(t) = c\left[(1+\alpha\Delta T(t)(\beta m(t) + (1-\beta))\exp\left(-\frac{D(t)}{\tau}\right) - (1+\alpha\Delta T(0)(\beta m(0) + (1-\beta)))\right], \tag{9}$$

and the derivative or slope of the degradation

$$\frac{dC}{dt} = c\exp\left(-\frac{D(t)}{\tau}\right)\left(\alpha\left(\frac{d\delta T}{dt} + \beta\frac{dm(t)}{dt}\right) - (1+\alpha\Delta T(t))\frac{1}{\tau}\frac{dD(t)}{dt}\right). \tag{10}$$

As τ is of the order of several years in the case of PMO6V-A the second term is small, and $\alpha\frac{d\delta T}{dt}$ dominates the slope over $\beta\frac{dm(t)}{dt}$ which is also much smaller. For VIRGO $\frac{d\delta T}{dt}$ is indeed explaining the annual modulation as shown in the lower plot of Fig. 2 and the modulation of the slope is dominated by the annual cycle of the temperature. From the slope fitting $\alpha = (9.96 \pm 0.24)10^{-4}$ is determined.

By replacing the integrals in Eq. 9 with sums and adding coefficients to be determined by fitting the following equation (replacing α, β, λ and R_0 accordingly) and with a_4 equal to $1/\tau$)

$$a_0 \left[(1 + a_1 \Delta T(t)(a_3 m(t) + (1 - a_3))) \exp\left(-a_4 \left(\sum_0^t \delta t_{\text{exp}} + a_5 \sum_0^t m(t_{\text{exp}}) - a_6 \sum_0^t \delta t_{\text{nexp}} \right) \right) \right]. \quad (11)$$

2 Corrections for the VIRGO PMO6V and DIARAD

The early behaviour of PMO6V is characterized by a rapid increase which is the result of a darkening of the illuminated part of the precision aperture, and hence a reduction of the reflected light into the baffle and an increase of a possible aperture heating. The darkening is confirmed by inspection of the apertures of the SOVA radiometers which were in space during the EURECA mission and brought back afterwards: the aperture of the less-exposed back-up instrument is dark and the operational one is bleached, but still darker than the part which was not irradiated at all. The bleaching seems to have a time constant much longer than the darkening and a corresponding correction may be included in the long-term degradation and it does not need to be concerned for the early increase. At first the explanation of this effect was difficult mainly because of its rather large value of about 500 ppm for PMO6V-A, 350 ppm for B, 590 ppm for ACRIM-I and about 1000 ppm for HF (Fröhlich, 2006) and an increase of the absorptivity of the cavity as an explanation is unrealistic because the total reflectivity of the cavity is only about 300 ppm. Also aperture heating is too small as model calculations show citep[][]Frohlich2010-2. So, the scattered light from the precision aperture into the baffle and back to the receiver could be an explanation, the amount of which obviously changes with the reflectivity of the precision aperture. This effect was also suspected to explain the large difference in absolute values of about 0.3 % between the classical radiometers HF, ACRIM, PMO6V and DIARAD and TIM on SORCE. However, the corresponding correction was measured by Brusa and Fröhlich (1986) with a laser illuminating the precision aperture and measuring the radiation scattered back through the aperture with a Silicon detector; the result was of the order of 350–500 ppm - no way to explain a 0.3 % influence. The energy reflected into the baffle is area wise more than 2.5 times higher than what is received by the cavity. With a reflectivity of 60% this means that the baffle receives about 40 mW which is mostly absorbed. Hence, the infrared radiation from the heated baffle would be important and can possibly explain the effect. Comparison at TRF of spare radiometers of PMO6V and ACRIM with a cryogenic radiometer have shown that, indeed, the amount of scattered and infrared radiation from the baffle is large enough to explain the scale difference (Kopp and Lean, 2011; Kopp et al., 2012). It is interesting, that DIARAD does not show an early increase and the recent TRF comparison confirm that it has also no effect of 'scattered' radiation. As both effects are related to the reflection at the primary aperture and the fact that DIARAD has a curved precision aperture which focuses the radiation falling on it back into the view-limiting aperture and thus out of the radiometer explains its non-sensitivity. The large contribution of an infrared radiation from the baffle means also that the air-vacuum ratio of the PMO6 radiometer is not only due to the non-equivalence produced by losses of the cavity to the surroundings. Brusa (1983) determined these effects in some detail and found that the difference of the air-vacuum ratio between PMO6 radiometers with a thick outer wall of the cavity was not as expected, namely substantially lower for the thick wall radiometer, but only slightly less than for the thin-wall types. This means that the air-vacuum ratio is indeed dominated by the 'scattered' light effect and not only due the non-equivalence as normally assumed.

The level-1 VIRGO data are essentially raw data, corrected for all known effects, such as electrical calibration, temperature, instrument-sun distance and radial velocity. The normal practice to correct level-1 data (Fig. 5) for degradation and other changes in space is based on the comparison of the measurements from the operational radiometers with those of the less exposed ones, the back-ups. For DIARAD this procedure is straightforward because the backup is exposed very little during the mission (about 10 days during the now 18 years in space) and can be assumed as having no degradation. The correction depends, however, on how the ratio DIARAD-R/L is determined. Up to version 6.002 this ratio was determined by IRMB (made available in the so-called ageing files) shown in Fig. 6 after smoothing as 'old from R/L. In spring 2013 IRMB stopped to produce this product and a new algorithm was developed, which is directly based on the DIARAD level-1 files from the VDC (VIRGO data center at Tenerife, operated by the IAC). As the left and right channels of DIARAD cannot be operated at the same time, the algorithm calculates the ratio (or difference) from the linearly interpolated DIARAD-L values during that day and the average of DIARAD-R, shown as 'new R/L and 'new R/L outliers on Fig. 6. For the PMO6V radiometers this procedure is complicated by the fact that the shutters of both radiometers could no longer operated after about 70 days in space and had to be replaced by opening and closing the covers at 8-hour intervals

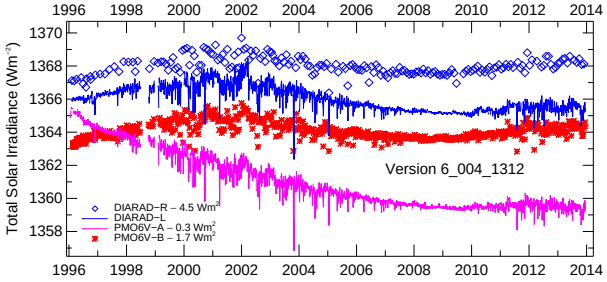

Figure 5: *Measurements (Level 1) of the two operational radiometers, PMO6V-A and DIARAD-L and their back-ups, PMO6V-B and DIARAD-R.*

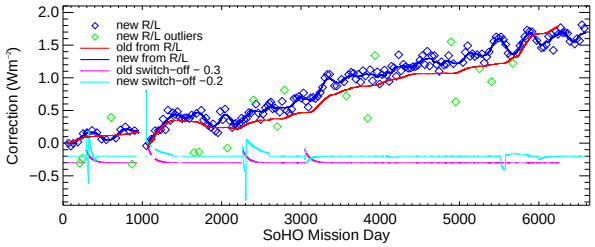

Figure 6: *Corrections of DIARAD-L from comparision with DIARAD-R for degradation and switch-offs for both versions, the 'old 6.002 and the 'new 6.004.*

(see e.g. Fröhlich et al., 1997). At the beginning of this new operational mode PMO6V-B was quite frequently exposed and thus these measurements need to be corrected for the early increase before they can be used to correct PMO6V-A. From mission days 83-218 the cover was normally closed and opened every 8 hours for 30 minutes, up to the SoHO vacation every 7 days and afterwards every 10 days. We will come back to how the correction of PMO6V-B are determined.

In order to apply the corrections from the rarely available values of DIA-R or PMO-B to the operational measurements one needs an interpolation scheme. In the versions up to 6.002 this interpolation was done by smoothing. As the degradation is modulated by the annual temperature change the interpolation should maintain also shorter periods. For version 6.004 the new algorithm is used based on splines (in IDL use the functions `spl_init` and `spl_interp`). The measured values of R−L or B−A are first spline-interpolated to provide a time series of daily values. These are smoothed with a boxcar over 151 days and the originally measured values R−L or B−A are replaced by the smoothed values. A new spline interpolation between these smoothed values yields then the values for the final corrections of L or A which now show, indeed, variations related to temperature. For DIARAD the result is shown on Fig. 6 as 'new from R/L. DIARAD has also some changes related to the switch-off of the experiment during the mission, which happened for 2 to 3 days six times during the 18-year operation due to Emergency Sun Re-acquisition (ECR) of SoHO and once due to a latch-up-induced switch-off of the VIRGO power supply. After the event in September 1996 it became clear that DIARAD showed a slow

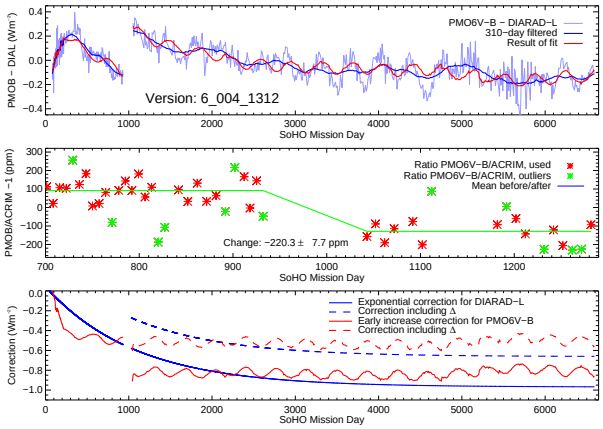

Figure 7: *The top panel shows the difference between PMO6V-B and DIARAD level-1.8 used to fit the early increase and exponential model, the middle panel the comparison of the corrected PMO6V-B with ACRIM-II to determine the change over the SoHO vacations, and the bottom panel the corrected data.*

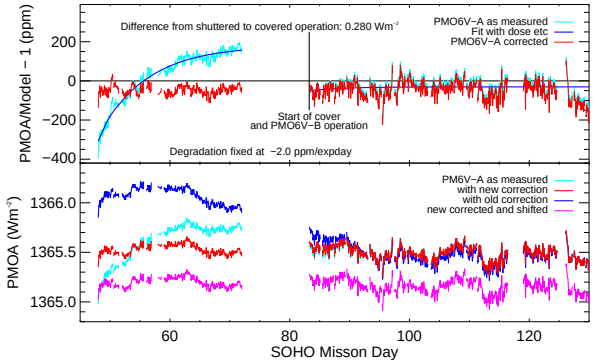

Figure 8: *Top panel: Ratio of the irradiance of PMO6V-A to a combination of the proxy model and DIARAD, which starts only at 7 February 1996. Apart from the correction due to the early increase, the change of absolute values due to change from shuttered to covered operation of -0.280 Wm^{-2} is also determined. Bottom panel: Corrected PMO6V-A values 'with new corrections compared to the former ones as 'with old corrections. Also shown are the shifted values as used in the further analysis which refer the absolute values to the first-light value.*

recovery after the experiment was switched on again and a similar recovery was identified after the SoHO vacations. The later events, however, were no longer as clear as the ones before. These changes were determined after each switch-on

by comparison with PMO6V-A at level 1 and also some glitches were found during the recovery time of a couple months. Both the corrections for versions up to 6.002 and for 6.004 are shown in Fig. 6 as 'old and 'new switch-off. With all these corrections the DIARAD level 1.8 values can be determined. After the SOHO vacations it became clear that the DIARAD must have also a non-exposure-dependent change of its sensitivity, both from comparison with PMO6V and other radiometers in space, and it was likely that this change can be modeled by an exponential. In version 6.002 and before this was performed by comparing the level 1.8 of PMO6V-A and DIARAD. In the present version the difference between the level 1.8 DIARAD and the level 1 PMO6V-B is fitted to the model (Eq. 11) for the early-increase for PMO6V-B and to an exponential for DIARAD. The coefficients for PMO6V-B are then used to correct it and by comparison with ACRIM the change over the SoHO vacations can be determined. The procedure and the results are shown in Fig. 7 and it is quite interesting that PMO6V-B does not show any significant change over the SoHO interruption, so the major part or probably all change of this difference is due to DIARAD. These changes may have the same reason as the long-term sensitivity change, namely a change of the thermal contact of the cavity to heat-flux meter (probably due to exposure to the space environment), because the area covered by electrical substitution heater is larger than the irradiated area by a factor of about 2.5. Normally these two area are the same size and coincident by design and hence, there is no influence of a change of the thermal resistance. With the coefficients of the exponential the final DIARAD level 2 values can now also be determined.

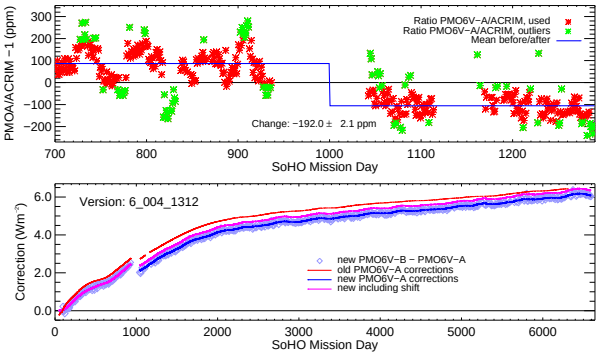

Figure 9: *The bottom panel shows the corrections for both versions, the 'old 6.002 and the 'new 6.004 of PMO-A from comparison with the corrected PMO-B and the top panel the comparison with ACRIM for the determination of the change over the gap.*

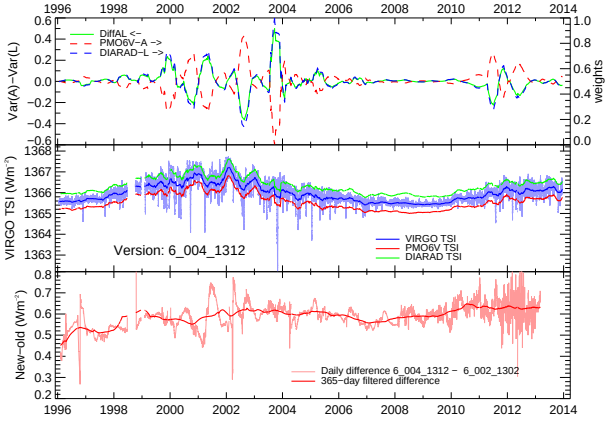

Figure 10: *The top panel shows the standard deviation of DIA-L and PMO-A as used to weigh each for the average VIRGO value. The middle panel shows the three final time series and the bottom panel the difference between the new version 6_004 and the old one 6_002.*

Before we can determine the level 2 PMO6V-A we need to correct the A values at the beginning for the early increase. The main part of the increase is during the shuttered operation which provides a reference to the original absolute calibration and later the change in calibration due the change in operation. For this early increase correction we need TSI values to compare with. As DIARAD starts at mission day 68 only, we expand these data with the proxy model to mission day 48, the start of the PMO-A. For fitting the model of Eq. 11 a further parameter is added, representing a degradation of 2 ppm/day typically. The result is shown in Fig. 8 and with the level 2 PMO-B series the corrections for PMO-A over the whole mission can be determined and interpolated by the method of splines to the hourly values as shown in Fig. 9 and the change over the SoHO interruption is determined by comparison with ACRIM (top plot). Again, the PMO-A has not changed during SOHO vacations similar to PMO-B.

VIRGO TSI is defined as the average of the PMO6V and DIARAD values and is determined by weighting. The weights are deduced from the difference of the variances, stddev^2 of PMO6V minus the one of DIARAD, each determined from a 81-day-running period and shown by the green line on the top panel of Fig. 10, smoothed with a 131-day boxcar. It is normalized in such a way that the absolute maximum is set to 0.5 and a positive difference means that the noise of PMO6V is higher and its weight correspondingly lower and a negative one that the noise of DIARAD is higher. So, weights from $0 \ldots 1$ are shown as red and blue dashed lines (with the left scale). On the other hand, DIARAD has in general less noise than PMO6V with e.g. the spikes during the keyholes due to the fact that still the original level 0–1 algorithm. For the

moment, it seemed more important to have an internally consistent way to produce the level 2 data, than improving on the noise of PMO6V. The new evaluation of level 0–1 is under way and will be available in due time.

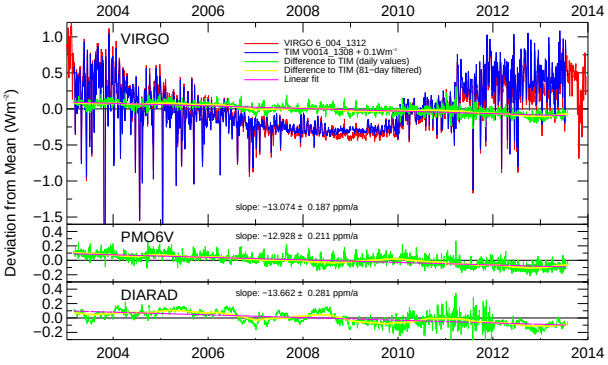

Figure 11: *The top panel shows the time series of VIRGO and TIM and their difference and the bottom panels the difference to PMO6V and DIARAD respectively. DIARAD shows less short-term noise than PMO6V, on the other hand PMO6V has less longer term deviations relative to TIM.*

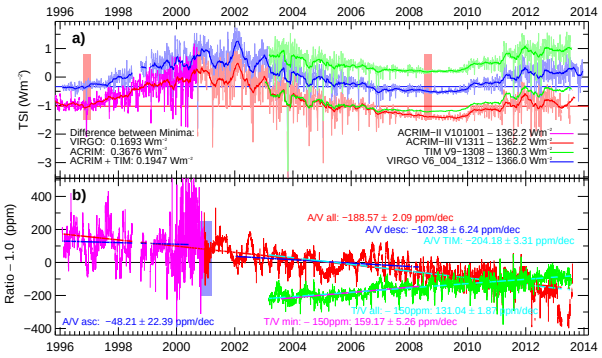

Figure 12: *VIRGO TSI is compared to ACRIM and TIM. The ACRIM values are on the scale of ACRIM 3 (version 1311). It is interesting to note that the slope relative to ACRIM for the whole period and for the TIM period are very similar although the time series is composed of ACRIM 2 and 3.*

As far as the absolute value is concerned VIRGO TSI is still on its original scale; the corresponding corrections are described in Fröhlich (2014). Besides the absolute value, the major results can be summarized as follows:

- Relative to TIM VIRGO TSI has a downward trend of 13.1 ± 1.9 ppm/a which would give yiels a difference of about 150 ppm over a solar cycle.
- Relative to ACRIM 3 VIRGO TSI has during the period of TIM an upward trend of 20.2 ± 1.9 ppm/a.
- VIRGO TSI has still the artefact during the keyholes of SOHO which are coming from the PMO6V data due to some inadequate temperature interpolation of missing values in the present level 0–1 evaluation. In general the PMO6V values have less medium- to long-term deviations relative to TIM than DIARAD, but the noise of PMO6V is higher. This is already seen in the comparison of DIARAD with PMO-B (see Fig. 7).

The new VIRGO TSI is certainly more reliable from an VIRGO-only point of view. No other time series are used besides ACRIM 2 to bridge the gap during the summer vacations of SOHO. However, we found that both PMO6V do not show a significant change - so *a posteriori* we could use this fact in the evaluation and leave out the tests with ACRIM 2.

From the final result we can determine the change of PMO6V over the SOHO gap as 13.3 ± 27.6 ppm and for DIARAD as 288.7 ± 15.7 ppm. These results can be used to determine the 1-σ uncertainty as less than 30 ppm due to the SSOHO gap and together with the uncertainty of the slope to TIM over cycle 24 of $12 \times 1.9 = 23$ ppm (from Fig. 11), an estimate of the uncertainty of the difference between the last two minima in 1996 and 2008 by summing the two components is 50 ppm or if we use the rms value 35 ppm. This value is lower than the 92 ppm reported in Fröhlich (2009) and makes the change between the minima of now 124 ppm more significant, but the value is smaller than the one reported in (Fröhlich, 2012) of 168 ppm for version 6_002_1110).

3 Where can you find the new data set?

This is work in progress and the web page is not yet updated and will then have a summary of this paper with the most important plots. The most recent daily and hourly VIRGO data are available with YYMM the corresponding update date from `ftp://ftp.pmodwrc.ch/pub/data/irradiance/virgo/TSI/virgo_tsi_d_v6_004_YYMM.dat` and `ftp://ftp.pmodwrc.ch/pub/data/irradiance/virgo/TSI/virgo_tsi_h_v6_`

004_YYMM.dat. The new PMOD composite with the new values of VIRGO is available from ftp://ftp.pmodwrc.ch/pub/data/irradiance/composite/DataPlots/composite_d41_64_YYMM.dat and ftp://ftp.pmodwrc.ch/pub/data/irradiance/composite/DataPlots/ext_composite_41_64_YYMM.dat.

This document is at: ftp://ftp.pmodwrc.ch/pub/Claus/VIRGO-TSI/VIRGO_TSI-vers64.pdf

References

R. W. Brusa. *Solar Radiometry*. PhD publ. no. 7181, Eidgenössische Technische Hochschule Zürich, Switzerland, 1983.

R. W. Brusa and C. Fröhlich. Absolute radiometers (PMO6) and their experimental characterization. Appl. Opt., 25: 4173–4180, 1986. doi: {10.1364/AO.25.004173}.

Deutschschweizerische Mathematik- und Physikkommission. *Formeln und Tafeln: Mathematik und Physik*. Orell Füssli Verlag Zürich, 7. edition, 1997.

C. Fröhlich. Solar irradiance variability since 1978: Revision of the PMOD composite during solar cycle 21. Space Sci. Rev., 125:53–65, 2006. doi: 10.1007/s11214-006-9046-5.

C. Fröhlich. Evidence of a long-term trend in total solar irradiance. A&A, 501:L27–L30, 2009. doi: {10.1051/0004-6361/200912318}.

C. Fröhlich. Total solar irradiance observations. *Surveys in Geophysics*, 33:453–473, 2012. doi: 10.1007/s10712-011-9168-5.

C. Fröhlich. VIRGO Radiometry: Update of the Characterization. Technical report, VIRGO Team, 7265 Davos Wolfgang, Switzerland, 2014. available from: ftp://ftp.pmodwrc.ch/pub/Claus/VIRGO-TSI/VIRGO_TSI-Char.pdf.

C. Fröhlich, D. Crommelynck, C. Wehrli, M. Anklin, S. Dewitte, A. Fichot, W. Finsterle, A. Jiménez, A. Chevalier, and H. J. Roth. In-flight performances of VIRGO solar irradiance instruments on SOHO. Sol. Phys., 175:267–286, 1997. doi: {10.1023/A:1004929108864}.

G. Kopp and J. L. Lean. A new, lower value of total solar irradiance: Evidence and climate significance. Geophys. Res. Lett., 38:L01706, 2011. doi: 10.1029/2010GL045777.

G. Kopp, A. Fehlmann, W. Finsterle, D. Harber, K. Heuerman, and R. Willson. Total solar irradiance data record accuracy and consistency improvements. *Metrologia*, 49:29, 2012. doi: 10.1088/0026-1394/49/2/S29.